A&A, 709, A139 (2026)
https://doi.org/10.1051/0004-6361/202557438

Astronomy & Astrophysics

First direct detection of an RR Lyrae star conclusively associated with an intermediate-age cluster

Cecilia Mateu[1,⋆], Bolivia Cuevas-Otahola[2], and Juan José Downes[1]

[1] Departamento de Astronomía, Instituto de Física, Universidad de la República, Iguá 4225, CP 11400 Montevideo, Uruguay
[2] Instituto de Astronomía, Universidad Nacional Autonoma de México, Ciudad Universitaria, Coyoacán, CP 04510, Ciudad de México, Mexico

Received 26 September 2025 / Accepted 19 March 2026

ABSTRACT

Context. RR Lyrae stars have long been considered unequivocal tracers of old (>10 Gyr) and metal-poor ([Fe/H] < −0.5) stellar populations. First, because these populations is where they are readily found and because, according to canonical stellar evolution models for isolated stars, these are the only populations where RR Lyrae are expected to exist. However, recent independent results are challenging this view and pointing to the existence of intermediate-age RR Lyrae (i.e. only about 2–5 Gyr old).
Aims. Our goal in this work is to provide direct evidence of the existence of intermediate-age RR Lyrae by searching for these stars in Milky Way open clusters, where the age association would be direct and robust.
Methods. We searched a catalogue of over 3000 open clusters with published kinematically associated member stars by cross-matching it against a compilation of the largest publicly available RR Lyrae surveys (*Gaia*, ASAS-SN, Pan-STARRS1, *Zwicky* Transient Facility, and OGLE-IV).
Results. We identified a star as a bona fide RR Lyrae variable and robust member of the 2–4 Gyr old Trumpler 5 cluster, based on its parallax and proper motions and their agreement with confirmed cluster members. We derived an extremely low probability ($0.049 \pm 0.013\%$) of the star being a background field RR Lyrae and we provide initial constraints on a possible binary companion based on its position in the colour-absolute-magnitude diagram.
Conclusions. As a current source of debate, the Trumpler 5 RR Lyrae star provides the most direct evidence to date of the existence of RR Lyrae stars at much younger ages than traditionally expected, adding to the mounting evidence supporting their existence.

Key words. binaries: general – stars: variables: RR Lyrae – open clusters and associations: general

1. Introduction

RR Lyrae (RRL) stars are classical pulsator core He-burning stars produced at the intersection of the instability strip and the horizontal branch (HB). A convenient combination of observational properties have made them an extremely popular tracer of Milky Way (MW) structure in the current era of deep, large-scale, synoptic photometric surveys. Due to their distinctive variability they are easily and reliably identified based on (multi-epoch) photometry alone; and being standard candles they provide individual distances with excellent precisions (down to a few per cent). Coupled with their high luminosities, this these features have made them ideal tracers of the 3D structure of our Galaxy and its surroundings (see e.g. Zhāng et al. 2025; Prudil et al. 2025; Cabrera-Gadea et al. 2025; Ngeow & Bhardwaj 2025; Medina et al. 2024; D'Orazi et al. 2024).

Recent studies are defying the canonical notion that RRLs are tracers of exclusively old and metal-poor populations (e.g. Catelan & Smith 2015; Smith 1995). In the first large-scale study of RRL kinematics in the MW using *Gaia* DR2 (Gaia Collaboration 2018), Iorio & Belokurov (2021) found a significant population of metal-rich RRLs ([Fe/H] $\gtrsim -0.5$ up to nearly solar) with kinematics resembling thin disc populations 2–5 Gyr-old, much colder and faster rotating than observed for disc populations at >10 Gyr, the age expected for canonical RRLs. Nearly simultaneously, in an independent study, Sarbadhicary et al. (2021) concluded that almost half (51%) the RRLs in the Large Magellanic Cloud (LMC) are associated with intermediate-age populations with ages from 1.2 to 8 Gyr. Their study was based on the delay time distribution (DTD) of RRLs, a measure of the number of objects per unit (initial) mass formed after a burst of star formation, inferred from the spatial distribution of RRLs and a map of the stellar age distribution across the LMC. Both studies are based on completely independent data and methods, with their results pointing towards the existence of intermediate-age populations of RRLs only a few Gyr old; thus, they would be much younger (and, in the case of the MW, also more metal-rich) than canonical stellar evolution models would predict. More recent studies of the kinematics of RRLs in the Galactic disc's warp (Cabrera-Gadea et al. 2025) and of the correlation of the kinematics of RRL and Mira stars of different ages determined via Mira's period-age relation (Zhāng et al. 2025) have further supported the kinematical intermediate age of thin-disc RRLs found by Iorio & Belokurov (2021).

Although these studies strongly support the existence of intermediate-age RRL stars, their conclusions rely on indirect age estimates and/or statistical inferences about the expected fraction of such stars. The only RRL so far identified as a 'young' object is the bulge field star OGLE-BLG-RRLYR-02792 found by Pietrzyński et al. (2012). It is also one of only two RRLs that have been robustly confirmed to be part of a binary

⋆ Corresponding author: cmateu@fcien.edu.uy

system (Hajdu et al. 2021). The star has a current mass of 0.26 $M_\odot$ and is found to be 5.4 Gyr old based on binary evolution models (Pietrzyński et al. 2012; Smolec et al. 2013). Pietrzyński et al. (2012) showed this mass is too low for the star to be undergoing core He-burning, calling it an RRL impostor and the prototype of a new 'binary evolution pulsator' class. These precedents highlight the need for a direct and unambiguous identification of individual RRLs associated with an intermediate-age cluster, where the age association is unequivocal and the non-variable population of the cluster can serve as a benchmark for atmospheric abundances to be compared against. Such objects will provide key constraints on the evolutionary channels currently proposed to explain the existence of these 'young' RRLs; for instance, via stellar population synthesis models, including binary evolution with mass transfer (Karczmarek et al. 2017; Bobrick et al. 2024), or via single stellar evolution with increased mass loss (Bono et al. 1997a,b).

In Cuevas-Otahola et al. (2025), we conducted a search for RRLs associated with intermediate-age clusters in the Magellanic Clouds (MCs), in an attempt to find direct evidence confirming the existence of these stars at such early ages. The search yielded 23 RRL possible members in ten clusters with ages from 2 to 8 Gyr. Given the large distance to the clusters, the current precision of *Gaia* DR3 proper motions is not yet enough to offer conclusive kinematic memberships and about half the RRLs are expected to be field contaminants from the MC's population, awaiting spectroscopic follow-up for radial velocities to confirm their memberships to the clusters.

In the MW, the vast majority of clusters found at ages younger than 8 Gyr are open clusters (OCs) whose masses are typically $< 10^3 M_\odot$ (with a handful of young massive clusters (YMCs) of higher masses, Portegies Zwart et al. 2010). The present-day formation rate (PTF) of 0.83 RRLs/10^5 $M_\odot$ found by Cuevas-Otahola et al. (2025) for clusters in that age range implies that only one in a few thousand clusters is statistically expected to host a single RRL and a search over a large sample of several thousand clusters is warranted. Such a search has become feasible thanks to *Gaia*, which has allowed for millions of stars to be catalogued as members of a vast number of OCs (over 5000), with kinematic membership probabilities robustly estimated based on parallax and proper motions (e.g. Hunt & Reffert 2023; Cantat-Gaudin et al. 2018, 2020). A quick estimate from the cluster masses reported by Hunt & Reffert (2024) and the Cuevas-Otahola et al. (2025) inferred rates yields a total mass of $\sim 4 \times 10^5 M_\odot$ for the 172 clusters in the age range from 1 to 8 Gyr, which implies ~2–3 RRLs could be lurking in the population of known Galactic OCs.

In this work, we present the first RRL star conclusively associated with an intermediate-age population: the 2–4 Gyr-old cluster Trumpler 5. This provides direct and model-independent evidence of the age of this young RRL star. In Sect. 2, we describe our search, conducted with a compilation of public RRL surveys cross-matched against the catalogue of stellar members associated with OCs from Hunt & Reffert (2023). Our search resulted in an initial sample of 15 candidates, out of which we confirm one star as a bona fide RRL. In Sect. 3, we show the star to be robustly identified as an RRL and as a cluster member by comparing it against cluster member's parallax, kinematics, and position in the colour-magnitude diagram (CMD) and by showing that it has an extremely low probability ($0.049 \pm 0.013\%$) of being a background field RRL. In Sect. 4, we discuss constraints on a possible binary companion based on its position in the CMD and the spectral energy distribution (SED), as well as on Trumpler-5 as a cluster that favours stellar evolution with mass transfer. We present our conclusions in Sect. 5.

2. Data

In this work, we use the OC census from Hunt & Reffert (2023) with mean cluster parameters from their Table 3 and members data from Appendix A of Hunt & Reffert (2024). In this latter work, the census from Hunt & Reffert (2023) was updated by including colour-magnitude diagram information in the cluster classification scheme and reporting extinction, age, and distance based on isochrone fitting, as well as the Jacobi radius and stellar mass for each cluster.

For the RRLs, we used the catalogue described in Cabrera-Gadea et al. (2025), which combines the *Gaia* DR3 SOS catalogue from Clementini et al. (2023), the Pan-STARRS1 (PS1) catalogue from Sesar et al. (2017a) and the ASAS-SN from Jayasinghe et al. (2019a,b), augmented with cross-matches against the *Zwicky* Transient Facility (ZTF) and the Optical Gravitational Lensing Experiment (OGLE) IV catalogues from Chen et al. (2020) and Soszyński et al. (2016), respectively, following the cross-matching strategy described in Cabrera-Gadea et al. (2025). The final GAPZO catalogue contains a total of 309 998 RRL stars spanning the full sky.

For our analysis, we cross-matched the GAPZO RRL catalogue by *Gaia* DR3 `source_id` against the OC member table from Hunt & Reffert (2024), keeping the 3530 clusters classified strictly as OCs (Type='o') to avoid globular clusters and moving groups, and with `CMDCl50`>= 0.5 and `CST`> 5 to keep only reliable OCs, as suggested by Hunt & Reffert (2023), and limiting our search to members within each cluster's tidal radius. This results in a sample of 3358 young (<1 Gyr) and 172 intermediate age clusters (1–8 Gyr), in which an initial number of 15 RRLs were identified as members of the same number of OCs. Out of these, 13 stars were identified as RRL by a single survey, one by two surveys (ZTF and *Gaia*) and the last one by all five surveys. Based on visual inspection of their light curves and position in the CMD, 14 out of the 15 stars were discarded based on their light curves (the majority were reclassified as eclipsing binaries) and/or their position in the CMD, as described in detail in Appendix A. In what follows, our discussion will focus on the last standing RRL star.

3. Results: The RRL star in Trumpler 5

Our search resulted in one star robustly identified as an RRL and as a member of an intermediate-age OC, the Trumpler 5 cluster. The RRL is identified as `source_id`=3326852328563919744 by *Gaia* DR3. *Gaia* DR3 astrometric parameters (Gaia Collaboration 2023) for the RRL and physical and astrometric parameters for the cluster from several sources are summarised in Table 1.

Anderson & Hunt (2025) recently conducted a similar search for variable stars in the Hunt & Reffert (2023) OC census by cross-matching against the *Gaia* DR3 Specific Objects Study (SOS) catalogues for different classes of variable stars and found two stars classified as RRLs by *Gaia*. Upon the inspection of their light curves and position on the CMD, the stars turned out to be likely eclipsing contact binaries and, consequently, the authors concluded no RRLs were found associated with OCs. However, their search was motivated by the study of much less luminous classes of variables and their sample was limited to clusters nearer than 2.5 kpc. We did not need to impose such a limitation here.

Table 1. Astrometric and physical parameters for the Trumpler 5 cluster and the RRL star.

Trumpler 5 cluster	
(RA, Dec)	(99.12705764, +9.45854713) deg
(l, b)	(202.82, +1.02) deg
Parallax	(0.302± 0.002) mas
pmRA*	(-0.618± 0.003) mas/yr
pmDec	(0.269± 0.002) mas/yr
Mass	$(2.46 \pm +0.17) \times 10^4\ M_\odot$
Age	2.2–4.2 Gyr
	2.5 Gyr (O25)
	$(2.17^{+1.00}_{-0.70})$ Gyr (H23)
	(3.5 ± 1.7) Gyr (D21)
	4.2 Gyr (CG20)
Distance	$(2.905^{+0.010}_{-0.009})$ kpc (H23)
	3.047 kpc (CG20)
[Fe/H]	−0.403 ± 0.006 (D15)
A_V	(1.71 ± +0.19) mag (H23)
r_t	(0.50 deg, 25.5 pc) (H23)
r_c	(0.077 deg, 3.9 pc) (H23)
r_{50}	(0.11 deg, 5.4 pc) (H23)
RRL	
`source_id`	3326852328563919744
(RA, Dec)	(98.90796904, 9.72592814) deg
(l, b)	(202.°48, 0.°95) deg
Parallax	(0.306 ± 0.028) mas
Distance (trig.)	2.95 ± 0.27 kpc (from parallax)
A_V	(1.65 ± 0.15) mag (G19)
	(1.503 ± 0.090) mag (L22)
pmRA*	(–0.627 ± 0.031) mas/yr
pmDec	(0.328 ± 0.026) mas/yr
G	(14.874 ± 0.012) mag
`ruwe`	1.1
BEP	1.3

Notes. O25 = Özdemir et al. (2025), H23 = Hunt & Reffert (2023), D21 = Dias et al. (2021), CG20 = Cantat-Gaudin et al. (2020), D15 = Donati et al. (2015), G19 = Green et al. (2019), L22 = Lallement et al. (2022).

3.1. A bona fide RRL

The star is consistently reported as an RR*ab* in all five surveys in the GAPZO catalogue. Table 2 summarises its main light curve parameters and Fig. 1 shows the star's light curves (top row) in the nine different filters for the four surveys with publicly available time series data. In all cases, the light curves show the typical sawtooth shape expected from its classification as an RRL of type *ab*. As observed in Fig. 1 and Table 2, amplitudes decrease as filters become redder, as expected for a pulsating star (e.g. Kinman & Brown 2010; Catelan & Smith 2015), except for the V-band amplitude from ASAS-SN. The location of the star in the period-amplitude diagram (bottom row) for all bands is consistent with the expectation from the period-amplitude anti-correlation in all eight bands available for *Gaia*, PS1 and OGLE-IV (only one band per survey is shown). For ASAS-SN, the relatively low V-band amplitude places the star below the main locus, however, the overall distribution for ASAS-SN RRL is much more scattered than usually observed, which is also reflected in a much weaker period-amplitude anti-correlation (Catelan & Smith 2015), in turn leading to lower amplitudes being more common in this catalogue. This suggests the low amplitude is more likely due to ASAS-SN amplitudes having a tendency to be underestimated, rather than it having a more physical explanation; for instance, based on the assumption the RRL might be a Blahzko star, which may have explained its lower amplitude. Therefore, we conclude the star's observed light curve, period, and amplitudes are typical for an RR*ab*.

Table 2. Period, light curve amplitudes, and (intensity averaged) mean magnitudes for the Trumpler 5 RRL.

Survey	Period (d)	Band	Amplitude (mag)	MeanMag (mag)
Gaia SOS	0.524806	*BP*	1.07	15.50
		G	0.82	14.87
		RP	0.69	14.09
ASAS-SN	0.524830	*V*	0.34	14.31
PS1	0.524815	*g*	1.07	15.84
		r	0.77	15.00
		i	0.61	14.53
		z	0.58	14.28
ZTF	0.524790	*r*	0.81	14.88
OGLE	0.524807	*I*	0.62	13.99

Notes. References are those provided for each survey in Sect. 2.

3.2. Kinematic cluster membership

Figure 2 shows the RRL star's position relative to cluster members from Hunt & Reffert (2024) in the sky and proper motion planes, in a parallax histogram, and in the colour–magnitude diagram (CMD), using *Gaia* bands (from left to right). As shown in the figure, the RRL lies within the cluster's tidal radius (by construction of our search) and its proper motions and parallax are in excellent agreement with the cluster's, supporting its likely membership at face value.

Our Trumpler 5 RRL was identified by Hunt & Reffert (2023) as a member of the cluster with a membership probability $p = 0.51$. The star had also been previously identified as a member of Trumpler 5 by Cantat-Gaudin et al. (2018, 2020) using *Gaia* DR2 and van Groeningen et al. (2023) using *Gaia* DR3, with probability 1 in all cases. All of these works compute membership probabilities by modelling the cluster in the same space of observables (sky, parallax, and proper motions) with a key difference being that membership probabilities from Hunt & Reffert (2023) were computed using HDBSCAN. According to the authors, their algorithm does not take into account observational errors and bases the assignment of probabilities on the proximity of a given star to the bulk of the cluster's population. This stands in contrast to the works of Cantat-Gaudin et al. (2018, 2020) and van Groeningen et al. (2023) whereby observational uncertainties are accounted for, which could explain the much lower membership probability found for this star by Hunt & Reffert (2023). Since this point is key, in Sect. 3.4, we revisit it and show that the probability of this star being a chance interloper of the thin-disc field population is extremely low.

Finally, an exhaustive search of major spectroscopic survey databases (DESI, LAMOST, and SDSS-IV) as well as using SIMBAD and VizieR yielded no available measurements for the star's line-of-sight velocity in the literature.

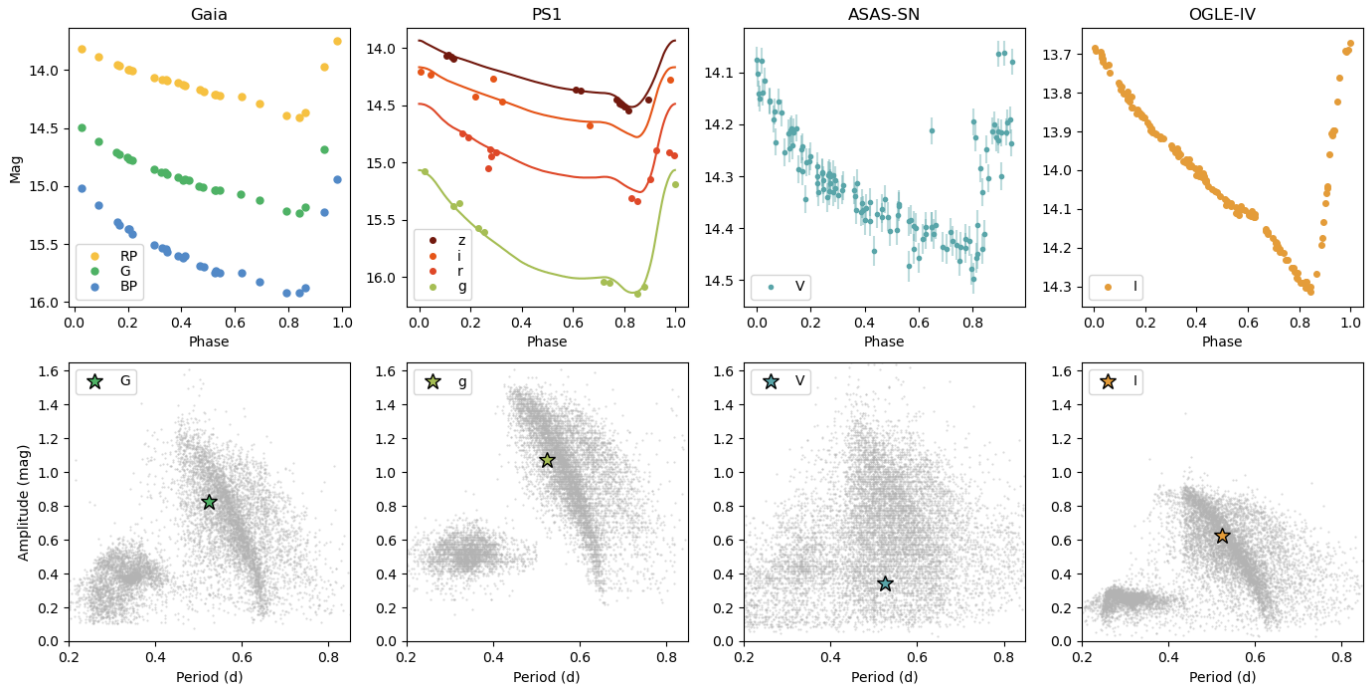

Fig. 1. Phase-folded light curves (*top*) and location of the Trumpler 5 RRL in the Period-Amplitude diagram (*bottom*) for the four surveys with publicly available time series data. *From left to right*: *Gaia* (Clementini et al. 2023), PS1 (Sesar et al. 2017b), ASAS-SN (Jayasinghe et al. 2019a), and OGLE-IV (Soszyński et al. 2016). In the bottom row, the location of the Trumpler 5 RRL (star symbol) is shown in comparison to RRLs from each survey in the selected band. See text for details. Error bars for the magnitudes are plotted in all panels in the top row but are smaller than the symbol size in all cases except for ASAS-SN.

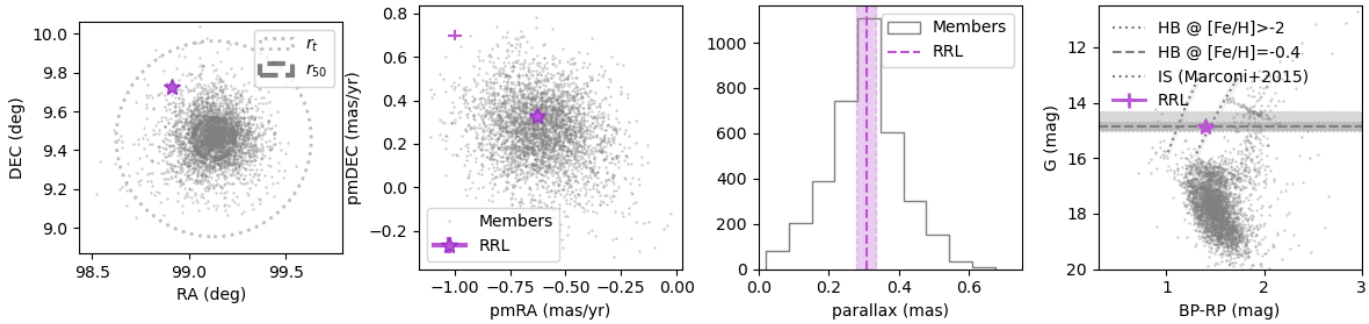

Fig. 2. Trumpler 5 RRL (star) and cluster members (light gray) shown (from left to right) in the plane of the sky (Dec versus RA), proper motions (pmDec versus pmRA), parallax, and *Gaia* CMD. In the first panel, r_t and r_{50} are shown with the dotted and dashed lines, respectively corresponding to the tidal radius and radius enclosing 50% of the members according to Hunt & Reffert (2023). In the fourth panel, the dotted lines correspond to instability strip (IS) limits from Marconi et al. (2015) for the cluster's metallicity; the dashed line shows the expected apparent G-band magnitude for the HB (from the empirical PLZ relation) at the cluster's metallicity ([Fe/H] = −0.4, Donati et al. 2015), and the star's parallax distance and extinction according to Green et al. (2019). The shading represents the uncertainty in the HB luminosity corresponding to the full range of (observed) RRL metallicities [Fe/H] ∈ [0., 2.0] dex and the uncertainties in the apparent magnitude and colour of the RRL are smaller than the star symbol. The agreement with the RRL's apparent magnitude is remarkable and the star lies right at the edge of the limits of the IS (see the discussion in Sect. 4.2.1).

3.3. Metallicity and location in the CMD

The star's photometric metallicity, estimated from the Fourier light curve ϕ_{31} parameter, has been reported by Clementini et al. (2023) as [Fe/H] = −0.44 ± 0.34, by Li et al. (2023) as −0.86 ± 0.33, by Muraveva et al. (2025) based on the *Gaia* DR3 G-band, and as −0.98 ± 0.45 and −0.71 ± 0.22 by He et al. (2025) from the ZTF g and i bands. The dispersion between the measurements, particularly of those inferred from the same data, shows that photometric metallicity estimates are still quite imprecise in an individual basis. In the last three cases, although the measurements show a slightly more metal-poor nature than that of the cluster, all estimates deviate by ≤1.4σ from the cluster's spectroscopic metallicity of [Fe/H] = −0.4 (Donati et al. 2015). We therefore assume the RRL's metallicity remains consistent with the cluster's within its uncertainties.

The RRL's position in the CMD is also shown in Fig. 2 (last panel), where a good agreement is found between the star's apparent G-band magnitude and that expected for the HB, assuming the cluster's metallicity of [Fe/H] = −0.403 ± 0.006 (Donati et al. 2015), its distance and extinction A_V = 1.65 from Green et al. (2019), and assuming the (empirical) absolute magnitude versus metallicity relation for the G band from Garofalo et al. (2022, Eq. (19)). The IS limits for the first overtone blue

edge (FOBE) and fundamental red edge (FRE) according to Marconi et al. (2015) for the cluster's metallicity are also shown. The limits provided by the authors in their Eqs. (3) and (4) for $\log T_{\rm eff}$, $\log L/L_{\odot}$ were transformed to the *Gaia* photometric system using the colour-$T_{\rm eff}$ transformation for Giants provided by Mucciarelli et al. (2021) in their Table 1 and a bolometric correction BC_G for the G-band at $T_{\rm eff}$ = 6500 K from the 2019 update of Table 5 from Pecaut & Mamajek (2013)[1].

Finally, we searched *Gaia* DR3 flags `ipd_frac_multi_peak` and `ipd_gof_harmonic_amplitude` for signs of potentially unresolved binarity (Lindegren 2018) but found none. Also the star's `ruwe` and `phot_bp_rp_excess_factor` (BEP) are normal, as shown in Table 1.

3.4. Not a background RRL star

Our argument that this a bona fide intermediate-age RRL star hinges on a reliable association to the cluster. A definitive association would require a measurement of the star's radial velocity, which is currently unavailable. In the meantime, we can assess how likely it is that our star is a chance interloper from the field population.

We quantified the probability that a field MW RRL has proper motions and parallax compatible with those of our star. For reference, within the cluster's projected tidal radius of ∼0.°5 there are only three other RRLs. Hence, a large window is needed to include enough RRLs for the background to be modelled properly, which already hints the likelihood of chance interlopers is very low. We selected a window that would include at least 2000 RRL, which resulted in a radius of ∼25°. Figure 3 shows the distribution of all field stars, field RRLs, cluster members and the RRL studied in this work. The distribution of field RRLs, while including both thin and thick disc contributions (e.g. Mateu & Vivas 2018; Prudil et al. 2020), is dominated by halo RRLs. Their bulk kinematics differ significantly from that of the cluster itself, as it is kinematically associated with the thin disc.

We used a Gaussian mixture to model the 3D distribution of proper motions and parallax of the background RRLs. We drew 500K random samples from the model and computed the fraction whose proper motions and parallax coincide with the RRL star's to within three times its uncertainties and estimated the probability and its error as the mean and standard deviations from 100 bootstrap realisations. This yielded a probability of $p = (0.012 \pm 0.003)\%$. The final probability that such a star was drawn at random in a sample of only four stars (i.e. the number of RRLs within the cluster's projected tidal radius) is given by the binomial probability of having one success in a sample of four draws when the probability of success is the value of p noted above. This yields a final probability of $(0.049 \pm 0.013)\%$ that the RRL is a chance interloper. Thus, it is clear the probability of the RRL in Trumpler 5 being a chance interloper is extremely low (1 in 2000) and we take the association based on proper motions and parallax as a very robust one, even without the radial velocity information.

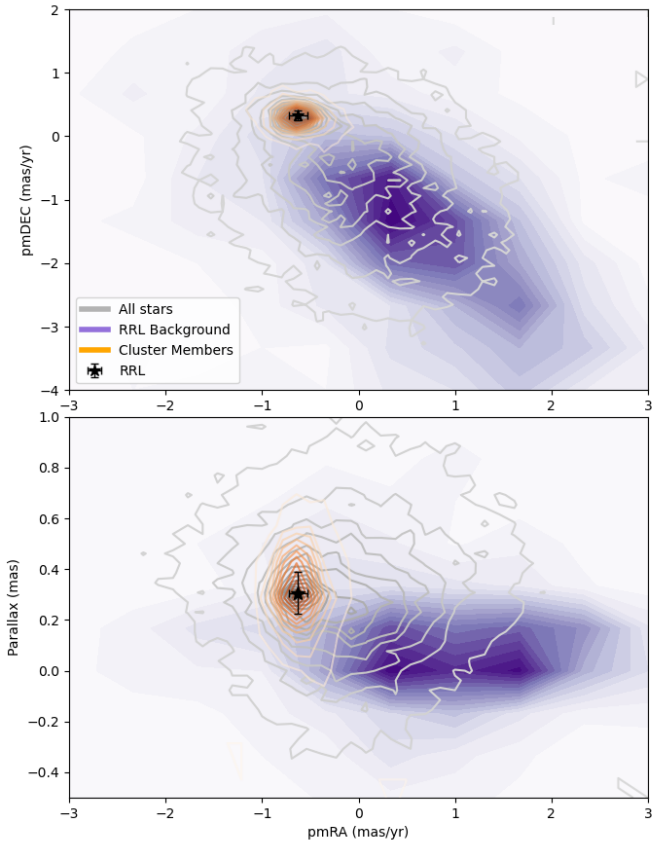

Fig. 3. Location of the Trumpler 5 RRL (black star) with respect to the field population in the proper motions (*top*) and parallax versus pmRA (*bottom*) planes. Iso-contours represent the density of cluster members (orange), all field stars (gray) within the cluster's tidal radius, and 2000 field RRL stars (violet) within in a FOV of 25°around the cluster. A similar result is found when using proper motion in declination (not shown). The analysis yields a final probability $(0.049 \pm 0.013)\%$ that the RRL is a chance interloper.

4. Discussion

4.1. Formation scenarios

We established that the RRL star is a robust member of the Trumpler 5 cluster. This provides a direct measurement of the RRL's age by virtue of its robust association to the cluster, independent of any assumptions on the nature and evolutionary formation channel.

The existence of an RRL star at such a young age (2–4 Gyr) challenges canonical stellar evolution channels and requires its progenitor to have lost a significant amount of mass for the star to have entered the IS and become an RRL pulsator. Two main avenues have been proposed for this: increased mass loss in single-star evolution models (Bono et al. 1997a,b; Taam et al. 1976) or binary interactions with mass transfer (Bobrick et al. 2024; Iorio & Belokurov 2021; Sarbadhicary et al. 2021).

Bono et al. (1997a,b) explored theoretical single-stellar evolution scenarios that would produce a metal-rich RRL via increased mass loss. Accounting for the increase in He abundance with metal content and using different prescriptions of mass loss at the RGB, their models are able to reproduce the formation of metal-rich RRLs up to solar metallicities for ages >2.5 Gyr and even younger for increased mass loss values. The zero-age HB luminosity found for these models ($\log L/L_{\odot} \sim 1.5$, $L \sim 31 L_{\odot}$) for ages > 2.5 Gyr and half the solar metallicity, is in agreement with more recent PLZ values for such a metal-rich RRL (e.g. Garofalo et al. 2022, see Fig. 4 below). The 'cause' of the increased mass loss, however, is not exclusively determined by the He enhancement and different mass loss prescriptions have been explored by the authors. For the Trumpler 5

[1] Available at `this URL`

RRL, about 1 $M_\odot$ would need to have been lost between the RGB and the HB stage for the star to reach the core He-burning stage with a core mass ∼0.5–0.6 $M_\odot$ reaching the IS. As discussed by Zhāng et al. (2025) in their Sect. 5.2 (and shown in their Fig. 9), such a large mass lost far exceeds the expectations from available wind mass loss estimates, which predict at most $\Delta M \sim 0.3 M_\odot$, based on metal-poor populations (Gratton et al. 2010; Savino et al. 2020; Tailo et al. 2021; Howell et al. 2024) or even lower for more metal-rich populations (Miglio et al. 2021). Additionally, the single stellar evolution effect responsible for such a high mass loss rate would need to have affected only the RRL, given that the red clump population of the cluster is found to be well described by stellar evolution models with normal prescriptions and He abundance (Özdemir et al. 2025). Since these tensions disfavour the single stellar evolution scenario, we turned our focus to the binary evolution scenario.

The second scenario is that of binary evolution, whereby the Trumpler 5 RRL could be a 'normal' RRL that is currently core He-burning after evolution and undergoing mass-transfer; alternatively, it could be a binary evolution pulsator or 'RRL impostor' such as the Pietrzyński et al. (2012) object. The pulsation properties predicted by Smolec et al. (2013) for these objects (red open squares in their Fig. 1) are roughly consistent with our star's period and amplitude. The BEP's light curve, however, is more irregular and less clearly saw-tooth shaped than our star, which has the light curve of a canonical RRab (see Fig. 1). The light curve dissimilarities do not seem to support this scenario; however, for a conclusive case to be made, models should be tailored to the specific properties of the Trumpler 5 RRL and, ideally, a dynamical estimate of the mass would be needed, requiring the star to be in a double-lined spectroscopic binary.

The lack of spectroscopic observations means that there is currently no direct evidence confirming (or ruling out) binarity. We analysed the *Gaia* `ruwe` parameter, which is consistent with a single star; however, this does not rule out low-mass and/or wide companions to which `ruwe` is not sensitive. The absence of visual companions only allows us to discard very wide binaries (an angular separation of ∼1″ corresponds to ∼1000 AU), which, in any case, would not be expected to have affected the evolution of the RRL. Next, we attempted to constrain the properties of a possible unresolved companion using photometry in two ways. First, we analysed the colour–absolute–magnitude diagram (CAMD) to estimate what type of companion could explain the position of the RRL star, slightly outside the limits of the IS. Second, we explore the presence of excess emission in the SED that could arise from a companion or from circumstellar material.

4.2. The binary evolution scenario

4.2.1. Location in the CAMD

Figure 4 shows the location of the Trumpler 5 RRL star in the CAMD using *Gaia* photometry. The absolute magnitude was computed from its intensity-averaged G-band magnitude from *Gaia* DR3 SOS (Clementini et al. 2023), its parallax distance of 2.95 ± 0.27 kpc computed including the -0.033 ± 0.002 mas offset correction found by Garofalo et al. (2022) for RRL stars. We kept this analysis focussed on the stars' trigonometric distance inferred from its parallax, rather than a photometric distance based on an empirical period-luminosity-metallicity (PLZ) relation, since this is a geometric distance completely independent of any assumptions on the star's nature as an RRL or of the validity of the PLZ for these unusual stars. Although metal-rich field RRL (which are probably also young, as mentioned in Sect. 1 and likely similar to the Trumpler 5 RRL) have been used as part of many calibration samples of PLZ relations (see e.g. Muraveva et al. 2018; Garofalo et al. 2022; Prudil et al. 2025), the extent of the validity of the PLZ relation for these objects is an aspect that remains to be explicitly tested. Hence, we opted to base our estimates of the RRL's location in the CAMD on its trigonometric (parallax-based) distance exclusively, allowing us to compare its derived luminosity (or absolute magnitude) to predictions from PLZs.

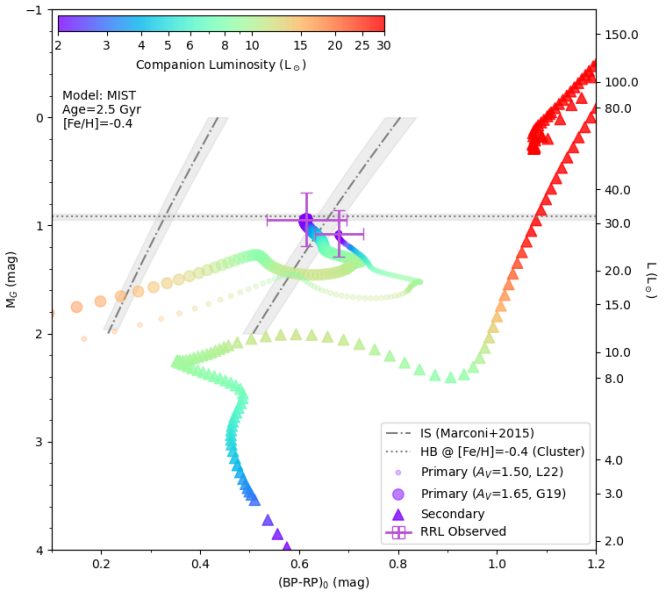

Fig. 4. CAMD for the cluster members (gray) and RRL (purple dots with error bars). Possible primary RRL stars are shown as coloured circles, and the corresponding secondary companions as triangles. The two tracks shown for primaries correspond to the G19 (large circles) and L22 extinctions (small circles). The colour scale represents the mass of the companion star. The IS limits for *RRab* from Marconi et al. (2015) and expected HB luminosity for the cluster's metallicity from the Garofalo et al. (2022) PLZ relation (as in Fig. 2) are shown by the dotted lines, the shaded areas correspond to their respective uncertainties.

The extinction correction turns out to be the largest source of uncertainty in the calculation of both M_G and colour because the cluster suffers from strong differential reddening (Özdemir et al. 2025), which varies with distance and along each line of sight. The figure shows the results obtained assuming an extinction $A_V = 1.65 \pm 0.15$ as predicted by the Green et al. (2019) map for the RRL's line of sight and its trigonometric distance, compared to an extinction of $A_V = 1.50 \pm 0.09$ mag predicted by the Lallement et al. (2022) dust map (hereafter L22)[2]. Extinction law coefficients from Fitzpatrick et al. (2019) were used for the conversion to the *Gaia* bands. According to G19's extinction the star is inside the IS and its luminosity is in remarkable agreement with the HB luminosity expected from the Garofalo et al. (hereafter G22 2022) empirical PLZ. According to L22's extinction, however, the star would be just past the red edge of the IS and slightly under-luminous compared to the HB from the G22 PLZ.

Constraints on the extinction can be derived from a similar comparison made taking advantage of the photometric information available for the star in different filters (summarised in Table 2). Figure 5 shows the difference between the observed

[2] See also Fig. B.1 for a more detailed comparison of L22 and G19.

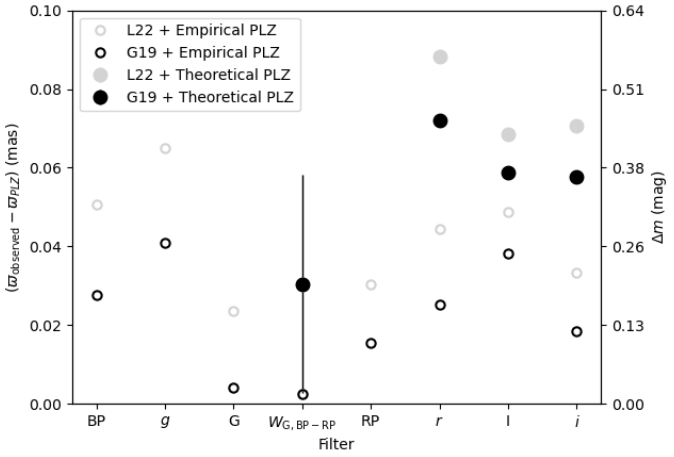

Fig. 5. Difference between the observed parallax and the parallax predicted from theoretical (filled circles) and empirical (open circles) PLZ relations for different photometric bands. The equivalent difference in magnitude is also represented in the right-hand axis. Results for the predicted parallax are shown for assumed extinctions from the G19 (black) and L22 (gray) dust maps. Since errors in this parallax difference are dominated by the uncertainty in the observed parallax, they are the same for all points and shown only for one band for guidance. Empirical PLZ relations used are from Narloch et al. (2024, Eq. (8)) for PS1 bands, from Prudil et al. (2024) for *I*, *BP*, and *RP* and from Garofalo et al. (2022) for the *G* and $W_{G,BP-RP}$ band. Theoretical relations used are from Marconi et al. (2021) for $W_{G,BP-RP}$, Marconi et al. (2015) for *I* and Marconi et al. (2022) for the LSST *r* and *i* bands (assumed here to match the PS1 bands, based on filter transmission curves for both surveys).

parallax and the corresponding prediction from empirical (open) and theoretical (filled) PLZ relations, both for the G19 (black) and L22 (gray) extinctions. This is also expressed equivalently in terms of a difference in magnitude, as shown by the right-hand axis. The figure shows the prediction from the empirical G22 PLZ for the reddening-free Wesenheit magnitude, $W_{G,BP-RP}$, is in remarkable agreement with the observed parallax. This result is also in best agreement with that obtained for the G band using the (larger) G19 extinction, instead of the L22 extinction which yields a systematic offset of $\gtrsim$0.02 mas. Therefore, in the following discussion, we have adopted the G19 extinction for the star.

Figure 5 also shows differences in the range 0.02–0.04 mas in the predicted parallax for empirical PLZs and systematically larger in the predictions from theoretical PLZs for all available photometric bands. If the Trumpler 5 RRL were not a real member of the cluster (and, instead, a normal field star either captured or simply coinciding in parallax and proper-motion with the cluster), the theoretically predicted PLZ parallax should be in agreement with the observed one. One aspect of particular interest is the discrepancy found for the theoretical predictions for the $W_{G,BP-RP}$ index; first because it is reddening-free, but also because this PLZ was empirically validated by Marconi et al. (2021) using *Gaia* DR2 astrometry for field RRL stars with robust metallicity information. In this band, the predicted parallax is ~0.03 mas smaller than the observed parallax[3]. The discrepancy observed for the *r*, *I*, and *i* bands is even larger $\gtrsim$0.06 mas (or ~20% in parallax or distance). Although there may be caveats due to this analysis being limited to a single object and the consistency still remains within the uncertainties, the systematic disagreement of the theoretical PLZ predictions found over the different bands and the smaller disagreement shown by empirical PLZs (based on RRL samples, including field stars likely of a similar nature to the Trumpler 5 RRL) are further arguments pointing against the possibility of the star being a normal RRL posing as a cluster member.

[3] Observed parallaxes already include the zero-point correction from G22. Not including this correction would even increase this discrepancy.

4.2.2. Constraints on binarity

To derive empirical constraints on the possible binarity of the star, we used its position on the CAMD to explore what the hypothetical secondary companions should be, so that the combined flux of the system would match the observed star, while keeping the primary inside the IS; these conditions would be required for the primary to develop the characteristic RRL pulsation (e.g. Smith 1995). Thus, we drew a secondary component from the normal cluster population and computed the primary's fluxes needed to reproduce the position of the observed star in the CAMD. This exercise required adopting an age for the cluster; however, as discussed by Özdemir et al. (2025), this choice is uncertain when relying on photometry alone due to strong differential extinction and the resulting age–metallicity–extinction degeneracy. Using NIR spectroscopy, Özdemir et al. derived atmospheric parameters for several giant stars in the cluster, performed differential-reddening corrections, and obtained an age of 2.5 Gyr using MIST isochrones (Dotter 2016; Choi et al. 2016). They also presented a strong argument for this age: the clearly observed gap caused by the blueward hook in the isochrones near the main-sequence turn-off, a feature found only in populations this young. Therefore, in what follows we adopt their estimate of 2.5 Gyr for the cluster age.

Figure 4 shows the resulting sequence of possible RRL primaries and their corresponding companions (triangles) that reproduce the observed position of the unresolved binary, according to the MIST models (Dotter 2016; Choi et al. 2016), for the G19 extinction (large circles). The result for the L22 extinction is also shown for comparison (small circles).

As the figure shows, main-sequence (MS) companions with luminosities $\lesssim 5 L_\odot$ are faint enough for the flux to be entirely dominated by the RRL primary and leave the star either in its observed position or slightly redder, still within the IS. More luminous MS companions, subgiant branch (SGB), and lower luminosity red giant branch (RGB) companions up to ~12 $L_\odot$ have been ruled out as, being bluer, they would require a cooler-and-redder primary outside the IS. As luminosity increases on the RGB, companions in the range ~12–18 $L_\odot$ start to be red enough to require a bluer primary inside the IS. Any companion more luminous than ~18 $L_\odot$ can also be ruled out as it would require a primary bluer than the blue edge of the IS. Further restrictions could be imposed on the companions knowing the observed star is an RR*ab*; thus, the primary must be on the red side of the IS. In addition, if the primary were to follow normal PLZ relations, the lower its luminosity, the shorter its pulsation period would be; again making it inconsistent with the observed properties of the star. These conclusions still hold for the lower extinction predicted by the L22 map, with minor changes to the luminosities of the possible companions. This analysis, therefore, supports either a low-luminosity ($\lesssim 5$ $L_\odot$) MS companion or no companion at all. This conclusion is consistent with the observed colour and magnitude of Trumpler 5's RRL.

The MS-companion scenario would be consistent with predictions from Bobrick et al. (2024), who used MESA stellar-population synthesis models including binary interactions to reproduce the production of young and metal-rich RRL stars.

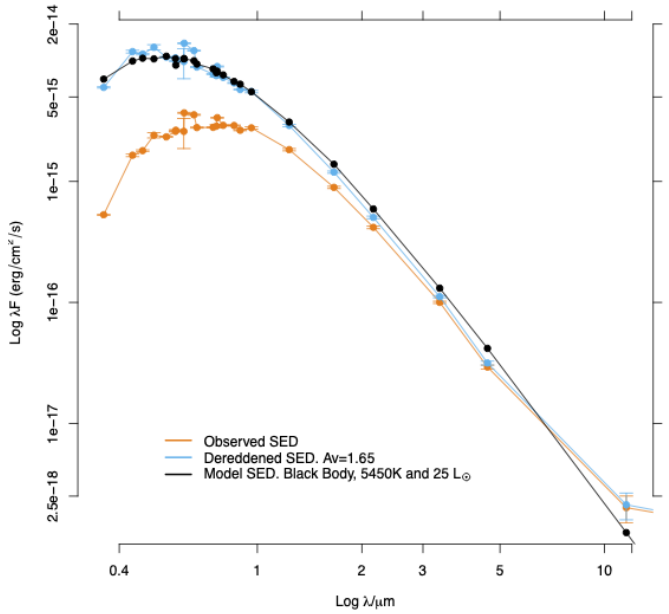

Fig. 6. SED of the RRL best fitted to a black body with $T_{\rm eff}$ = 5450K and $L = 25 L_{\odot}$. It includes magnitudes in 24 pass-bands from 2MASS, *Gaia* DR3, HST/ACS, IPHAS, PS1, SDSS, and WISE surveys. The SED was de-reddened by A_V = 1.65 and the extinction law from Fitzpatrick (1999) and Indebetouw et al. (2005).

In their simulations, binary-made RRL stars are formed from evolved stripped-RGB stars and have surviving MS companions with masses between 0.65 and 1.9 $M_{\odot}$ and luminosities $15 \lesssim L/L_{\odot} \lesssim 35$. Initial masses for binary-made RRL stars are found to be in the range 0.95–2 $M_{\odot}$ with mild mass ratios between 1.0 and 1.55. Because the primary is the star that becomes an RRL after ascending the RGB, its initial mass correlates with the age of the population. Since the mass ratios do not span a very broad range, Bobrick et al. (2024) pointed out that the secondary mass is also roughly correlated with age, with systems younger than 3 Gyr having companion masses larger than 1 $M_{\odot}$ and luminosities of $L > 1.5\ L_{\odot}$. This would be consistent with the Trumpler 5 RRL and G19 extinction and with luminosities at the higher end of the range predicted by Bobrick et al. (2024). It should be noted, however, that alternative scenarios of binary-made RRL formed after the binary system merges during the common envelope phase are also possible (Mateu et al., in prep.). Quantitative predictions and the relative efficiency of these channels are being tested as they depend on binary evolution parameters difficult to be constrained, such as the critical values for mass transfer stability and mass loss parameters, among others.

Finally, we also explored the possible existence of an IR excess, based on the SED of the star. Figure 6 shows the de-reddened SED for the RRL star built using the VOSA tool (Bayo et al. 2008) and available photometry from the literature over the wavelength range $0.36 \lesssim \lambda/\mu m \lesssim 11$. The SED displays a good fit to a single blackbody of $T_{\rm eff}$ = 5450 K with a luminosity of $L = 25\ L_{\odot}$ obtained when fitting only the optical wavelengths ($\lambda \lesssim 1.2$ μm), and the same result is found when fitting over the full wavelength range. This result rules out a luminous RGB companion and also suggests the absence of IR excesses up to $\lambda \lesssim 11$ μm from circumstellar material. The best fit to a two-blackbody model results in two indistinguishable components with the same temperature and half the luminosity each. Although the result supports the $T_{\rm eff}$ value that was previously found, it is not sensitive to companions with luminosities well below that of the RRL star, as the resulting changes are comparable to the photometric uncertainties. We note that available interferometric observations with angular resolutions and sensitivity to resolve even faint companions at angular distances of tenths of *mas* could probe for companion at distances from 30 to 300 AU.

In summary, the observed RRL is with the luminosity of a normal RRL, based on expectations for the HB luminosity from existing empirical PLZ relations and inconsistent with predictions from theoretical PLZs. Its position in the CAMD would be consistent either with no companion or with MS companions with luminosities up to ~5$L_{\odot}$, in agreement with predictions from the binary interaction models by Bobrick et al. (2024).

4.3. A binary-friendly cluster

The Trumpler 5 RRL was also identified by Rain et al. (2021) as a member of this cluster using the OC members from Cantat-Gaudin et al. (2018, 2020), and classified it as a so-called yellow straggler star (YSSs), one of the two found in that cluster. In their work, YSSs are defined as stars redder than the main sequence turn-off, bluer than the red giant branch, and more luminous than the subgiant branch; these conditions are indeed met by our star. In addition to the possibility of them being unresolved binaries whose combined fluxes place them in the YSS locus (Rain et al. 2021; Mermilliod et al. 2007), we note that YSSs are of special interest since it has also been proposed they may have been formed by binary mergers, collisions, and/or mass transfer from a red giant companion (Landsman & Stecher 1997; Landsman & Simon 1998; Leiner et al. 2016).

Rain et al. (2021) also found 103 blue straggler stars (BSSs) in Trumpler 5, making it the OC with the largest absolute population of BSSs and the 8th in terms of its relative fraction, calculated as the fraction of BSSs relative to main sequence stars up to 1 mag below the turn-off. The correlation between the fraction of BSSs and the binary fraction of a population observed in open and globular clusters, as well as in dwarf galaxies (e.g. Ferraro et al. 2026; Momany 2015) implies Trumpler 5 hosts a relatively large population of binaries in comparison to other OCs. If binary evolution with mass transfer is indeed a viable evolutionary path for RRLs to be produced at intermediate ages, the relatively large mass of Trumpler 5 (>24 000 $M_{\odot}$) combined with a comparatively large binary fraction could arguably 'conspire' favourably for the cluster to have produced a binary-evolution RRL (despite how inefficient this mechanism might prove to be).

It should also be noticed that Trumpler 5 is an atypical OC, being older and more metal-poor than typical OCs (Özdemir et al. 2025), and exhibiting a mass that is higher than the canonical mass of OCs (Portegies Zwart et al. 2010). Trumpler 5 is a dynamically evolved cluster as shown by an analysis of the profile of its BSSs (Rain et al. 2020), with a mass resembling that of a low-mass YMC, leading to the possibility that it could be a transition cluster between OC and YMC, when considering OCs as the low-mass end of YMCs (Bastian 2016).

5. Conclusions

In this work we provide the first conclusive association of an RRL to an intermediate-age star cluster: the 2–4 Gyr-old Trumpler 5. This provides the first direct measurement of an intermediate-age RRL's age, independent of any assumptions

on the nature of the star or its possible evolutionary formation channel.

We have shown the star to be a bona fide RRL, identified independently and consistently by five RRL surveys: *Gaia* DR3 SOS, ASAS-SN, PS1, ZTF, and OGLE-IV. Its full information, as well as the cluster's, is provided in Table 1. The star was robustly identified as a member of the Trumpler 5 cluster by Hunt & Reffert (2024); Cantat-Gaudin et al. (2018) and Cantat-Gaudin et al. (2020), it is located within the cluster's tidal radius, and its proper motions and parallax are in remarkable agreement with the cluster's members. Its observed apparent G-band magnitude is consistent with the expectation from empirical RRL PLZ relations for the HB at the cluster's metallicity and at the star's distance and extinction according to the Green et al. (2019) dust map. Based on the parallax and proper motion distribution of field RRL stars and the total number of field RRLs observed within the cluster's tidal radius (3), we have shown the RRL to have a probability of $0.049 \pm 0.013\%$ of randomly sharing the cluster's parallax and proper motion to within three times the star's uncertainties. This result implies a very low chance of the RRL being a chance interloper. Given the size of the cluster sample (>3K OCs) searched in this work (Hunt & Reffert 2024), having observed one RRL in the 1–8 Gyr age range, implies a frequency of 0.25×10^{-5} $M_\odot$ RRL. This is in agreement, to within Poisson noise, with the ∼2 RRL expected from the $0.2 \pm 0.2 \times 10^{-5}$ $M_\odot$ PTF results obtained by Cuevas-Otahola et al. (2025) from LMC and SMC clusters, and with the $\sim 0.1 \times 10^{-5}$ $M_\odot$ rate predicted by binary evolution models from Bobrick et al. (2024).

Finally, although this is not firmly conclusive due to the large extinction uncertainties, we explored possible constraints on a binary companion based on the CAMD and the star's SED. With the assumed extinction ($A_V = 1.65$) from the G19 dust map, the star lies inside the IS and has a luminosity consistent with predictions from empirical PLZ relations for the G and $W_{G,BP-RP}$ bands. Theoretical PLZs are found to predict systematically smaller parallaxes than observed and also compared to predictions from empirical PLZs in all available bands, while also disfavouring the possibility of the star being a normal background star posing as a cluster member. Given its position in the CAMD, the RRL is consistent with being a single star or, if in a binary, the most likely scenario would require the secondary to be a low-luminosity MS star ($L < 5L_\odot$). In addition, SGB or low-luminosity RGB companions are also possible, but would require a significantly under-luminous RRL. Finally, the star's SED analysed with VOSA showed no signs of an IR excess from circumstellar material up to 11 μm.

The association of an RRL star to Trumpler 5, a decidedly intermediate-age simple stellar population, is the most direct evidence so far of the existence of these 'young' RRLs and lends firm support to the evidence that has been systematically accumulating toward the existence of RRL stars at these unusual ages, both in the MW and LMC (Iorio & Belokurov 2021; Sarbadhicary et al. 2021; Zhāng et al. 2025; Cabrera-Gadea et al. 2025; Cuevas-Otahola et al. 2025).

Acknowledgements. The authors would like to thank the anonymous referee for a constructive discussion and useful suggestions. CM is delighted to thank Pau Ramos and Danny Horta for useful discussions and early readings of the manuscript, as well as Giuliano Iorio, Alexey Bobrick, Valentina D'Orazi, Zdenek Prudil and Tatiana Muraveva from the Synergy Team for useful comments. JJD and BCO acknowledge support from the RDT funding from Universidad de la República, Uruguay. This work has made use of data from the European Space Agency (ESA) mission *Gaia* (https://www.cosmos.esa.int/gaia), processed by the *Gaia* Data Processing and Analysis Consortium (DPAC, https://www.cosmos.esa.int/web/gaia/dpac/consortium). Funding for the DPAC has been provided by national institutions, in particular the institutions participating in the *Gaia* Multilateral Agreement.
Software: Astropy (Astropy Collaboration 2018), Matplotlib (Hunter 2007), Numpy (Walt et al. 2011), Jupyter (Kluyver et al. 2016), TOPCAT (Taylor 2005, 2006), dustmaps (Green 2018).

References

Anderson, R. I., & Hunt, E. L. 2025, A&A, 700, L13
Astropy Collaboration (Price-Whelan, A. M., et al.) 2018, AJ, 156, 123
Bastian, N. 2016, in EAS Publications Series, 80–81, eds. E. Moraux, Y. Lebreton, & C. Charbonnel, 5
Bayo, A., Rodrigo, C., Barrado Y Navascués, D., et al. 2008, A&A, 492, 277
Bobrick, A., Iorio, G., Belokurov, V., et al. 2024, MNRAS, 527, 12196
Bono, G., Caputo, F., Cassisi, S., Castellani, V., & Marconi, M. 1997a, ApJ, 479, 279
Bono, G., Caputo, F., Cassisi, S., Incerpi, R., & Marconi, M. 1997b, ApJ, 483, 811
Cabrera-Gadea, M., Mateu, C., & Ramos, P. 2025, A&A, 701, A136
Cantat-Gaudin, T., Jordi, C., Vallenari, A., et al. 2018, A&A, 618, A93
Cantat-Gaudin, T., Anders, F., Castro-Ginard, A., et al. 2020, A&A, 640, A1
Catelan, M., & Smith, H. A. 2015, Pulsating Stars, 1st edn. (Weinheim, Bergstr: Wiley-VCH)
Chen, X., Wang, S., Deng, L., et al. 2020, ApJS, 249, 18
Choi, J., Dotter, A., Conroy, C., et al. 2016, ApJ, 823, 102
Clementini, G., Ripepi, V., Garofalo, A., et al. 2023, A&A, 674, A18
Cuevas-Otahola, B., Mateu, C., Cabrera-Ziri, I., et al. 2025, MNRAS, 541, 1434
Dias, W. S., Monteiro, H., Moitinho, A., et al. 2021, MNRAS, 504, 356
Donati, P., Cocozza, G., Bragaglia, A., et al. 2015, MNRAS, 446, 1411
D'Orazi, V., Storm, N., Casey, A. R., et al. 2024, MNRAS, 531, 137
Dotter, A. 2016, ApJS, 222, 8
Ferraro, F. R., Lanzoni, B., Vesperini, E., et al. 2026, Nat. Commun., 17, 768
Fitzpatrick, E. L. 1999, PASP, 111, 63
Fitzpatrick, E. L., Massa, D., Gordon, K. D., Bohlin, R., & Clayton, G. C. 2019, ApJ, 886, 108
Gaia Collaboration (Brown, A. G. A., et al.) 2018, A&A, 616, A1
Gaia Collaboration (Vallenari, A., et al.) 2023, A&A, 674, A1
Garofalo, A., Delgado, H. E., Sarro, L. M., et al. 2022, MNRAS, 513, 788
Gratton, R. G., Carretta, E., Bragaglia, A., Lucatello, S., & D'Orazi, V. 2010, A&A, 517, A81
Green, G. M. 2018, J. Open Source Softw., 3, 695
Green, G. M., Schlafly, E., Zucker, C., Speagle, J. S., & Finkbeiner, D. 2019, ApJ, 887, 93
Hajdu, G., Pietrzyński, G., Jurcsik, J., et al. 2021, ApJ, 915, 50
He, S.-X., Huang, Y., Li, X.-Y., et al. 2025, ApJS, 278, 2
Howell, M., Campbell, S. W., Stello, D., & De Silva, G. M. 2024, MNRAS, 527, 7974
Hunt, E. L., & Reffert, S. 2023, A&A, 673, A114
Hunt, E. L., & Reffert, S. 2024, A&A, 686, A42
Hunter, J. D. 2007, Comput. Sci. Eng., 9, 90
Indebetouw, R., Mathis, J. S., Babler, B. L., et al. 2005, ApJ, 619, 931
Iorio, G., & Belokurov, V. 2021, MNRAS, 502, 5686
Jayasinghe, T., Stanek, K. Z., Kochanek, C. S., et al. 2019a, MNRAS, 486, 1907
Jayasinghe, T., Stanek, K. Z., Kochanek, C. S., et al. 2019b, MNRAS, 485, 961
Karczmarek, P., Wiktorowicz, G., Iłkiewicz, K., et al. 2017, MNRAS, 466, 2842
Kinman, T. D., & Brown, W. R. 2010, AJ, 139, 2014
Kluyver, T., Ragan-Kelley, B., Pérez, F., et al. 2016, in Positioning and Power in Academic Publishing: Players, Agents and Agendas, eds. F. Loizides, & B. Schmidt (IOS Press), 87
Lallement, R., Vergely, J. L., Babusiaux, C., & Cox, N. L. J. 2022, A&A, 661, A147
Landsman, W., & Simon, T. 1998, in American Astronomical Society Meeting Abstracts, 193, 37.03
Landsman, W., & Stecher, T. P. 1997, in American Institute of Physics Conference Series, 408, The Ultraviolet Universe at Low and High Redshift, ed. W. H. Waller, 390
Leiner, E., Mathieu, R. D., Stello, D., Vanderburg, A., & Sandquist, E. 2016, ApJ, 832, L13
Li, X.-Y., Huang, Y., Liu, G.-C., Beers, T. C., & Zhang, H.-W. 2023, ApJ, 944, 88
Lindegren, L. 2018, Gaia technical note GAIA-C3-TN-LU-LL-124
Marconi, M., Coppola, G., Bono, G., et al. 2015, ApJ, 808, 50
Marconi, M., Molinaro, R., Ripepi, V., et al. 2021, MNRAS, 500, 5009
Marconi, M., Molinaro, R., Dall'Ora, M., et al. 2022, ApJ, 934, 29
Mateu, C., & Vivas, A. K. 2018, MNRAS, 479, 211
Medina, G. E., Muñoz, R. R., Carlin, J. L., et al. 2024, MNRAS, 531, 4762

Mermilliod, J. C., Andersen, J., Latham, D. W., & Mayor, M. 2007, A&A, 473, 829
Miglio, A., Chiappini, C., Mackereth, J. T., et al. 2021, A&A, 645, A85
Momany, Y. 2015, in Astrophysics and Space Science Library, 413, eds. H. M. J. Boffin, G. Carraro, & G. Beccari, 129
Mucciarelli, A., Bellazzini, M., & Massari, D. 2021, A&A, 653, A90
Muraveva, T., Delgado, H. E., Clementini, G., Sarro, L. M., & Garofalo, A. 2018, MNRAS, 481, 1195
Muraveva, T., Giannetti, A., Clementini, G., Garofalo, A., & Monti, L. 2025, MNRAS, 536, 2749
Narloch, W., Hajdu, G., Pietrzyński, G., et al. 2024, A&A, 689, A138
Ngeow, C.-C., & Bhardwaj, A. 2025, AJ, 169, 156
Özdemir, S., Afşar, M., Sneden, C., et al. 2025, A&A, 699, A208
Pecaut, M. J., & Mamajek, E. E. 2013, ApJS, 208, 9
Pietrzyński, G., Thompson, I. B., Gieren, W., et al. 2012, Nature, 484, 75
Portegies Zwart, S. F., McMillan, S. L. W., & Gieles, M. 2010, ARA&A, 48, 431
Prudil, Z., Dékány, I., Grebel, E. K., & Kunder, A. 2020, MNRAS, 492, 3408
Prudil, Z., Kunder, A., Dékány, I., & Koch-Hansen, A. J. 2024, A&A, 684, A176
Prudil, Z., Debattista, V. P., Beraldo e Silva, L., et al. 2025, A&A, 699, A349
Rain, M. J., Carraro, G., Ahumada, J. A., et al. 2020, AJ, 161, 37
Rain, M. J., Ahumada, J. A., & Carraro, G. 2021, A&A, 650, A67
Sarbadhicary, S. K., Heiger, M., Badenes, C., et al. 2021, ApJ, 912, 140
Savino, A., Koch, A., Prudil, Z., Kunder, A., & Smolec, R. 2020, A&A, 641, A96
Sesar, B., Hernitschek, N., Dierickx, M. I. P., Fardal, M. A., & Rix, H.-W. 2017a, ApJ, 844, L4
Sesar, B., Hernitschek, N., Mitrović, S., et al. 2017b, AJ, 153, 204
Smith, H. A. 1995, RR Lyrae Stars, (Cambridge University Press)
Smolec, R., Pietrzyński, G., Graczyk, D., et al. 2013, MNRAS, 428, 3034
Soszyński, I., Udalski, A., Szymański, M. K., et al. 2016, Acta Astron., 66, 131
Taam, R. E., Kraft, R. P., & Suntzeff, N. 1976, ApJ, 207, 201
Tailo, M., Milone, A. P., Lagioia, E. P., et al. 2021, MNRAS, 503, 694
Taylor, M. B. 2005, in Astronomical Society of the Pacific Conference Series, 347, Astronomical Data Analysis Software and Systems XIV, eds. P. Shopbell, M. Britton, & R. Ebert, 29
Taylor, M. B. 2006, in Astronomical Society of the Pacific Conference Series, 351, Astronomical Data Analysis Software and Systems XV, eds. C. Gabriel, C. Arviset, D. Ponz, & S. Enrique, 666
van Groeningen, M. G. J., Castro-Ginard, A., Brown, A. G. A., Casamiquela, L., & Jordi, C. 2023, A&A, 675, A68
Walt, S. v. d., Colbert, S. C., & Varoquaux, G. 2011, Comput. Sci. Eng., 13, 22
Zhāng, H., Iorio, G., Belokurov, V., et al. 2025, MNRAS, 544, 2493

Appendix A: Discarded stars

The search for RRL members in OCs yielded an initial sample of fifteen stars. Here we discuss the fourteen stars which we discarded as misclassified RRLs, mainly based on the appearance of their phase-folded light curves and/or position in the CAMD. Figure A.1 shows the phase-folded light curves for all the time series publicly available from *Gaia*, ASAS-SN, PS1 and OGLE-IV for these stars. In this plot, stars C13 and C14 were identified as RRLs by ZTF alone. Since the ZTF time series are not available, we show the *Gaia* DR3 for C13. We were unable to find any time series information for star C14, hence it is not shown in Fig. A.1. Figure A.2 shows the proper motion plane, parallax histogram, CAMD and Period-Amplitude diagram for the star of interest (purple star) and cluster members from Hunt & Reffert (2023), similarly to Fig. 2. Table A.1 summarises the available light curve information for the discarded stars.

Since the RRLs we are interested in could belong to unresolved binaries we should not, a priori, rule out stars that lie outside the IS. We can, however, discard any stars below the expected HB luminosity since an unresolved binary can only be more luminous than the RRL, assuming it has a 'normal' luminosity. The position in the CAMD of Fig. A.2 for several stars (e.g. C5, C6, etc.) places them well below the HB and, in many cases, directly on the MS. These cases are denoted as below-HB/MS in the comments of Table A.1 as reasons for the stars to be discarded from our sample. In what follows we describe the criteria used to discard each star, also summarised in Table A.1.

Stars C1–C4, show the characteristic light curves of contact or semi-detached eclipsing binaries (W UMa/EW and βLyr/Eβ), consistent with their position on or near the MS as seen in the CAMD of Fig. A.2. Star C5 has a very noisy light curve and is placed well below the MS. Stars C6, C8, C9, C10 and C11 have reasonably well behaved light curves, but too short amplitudes much more consistent with being either δ Scuti stars or eclipsing binaries (EB), the latter being more consistent with their position in the MS but outside the IS, in the CAMD. Star C7 is bluer than the IS and more luminous than the HB, which would make it a good candidate, except for its extremely low amplitude, particularly for its period, and the significant gap in its light curve. This star might be worth revisiting, but for now it is discarded as a possible EB. Stars C12 and C13 show almost constant light curves with a few deviated points, usually characteristic of detached eclipsing binaries (Algol/EA). This is indicated with the corresponding variability classification in the comments of Table A.1. Finally, star C14 has a very short amplitude and is located right at the MS, well below the HB. Although it is the only star without time series data available, its very short amplitudes and location in the CAMD make it likely to be an EB.

Table A.1. Stars discarded as misclassified RRLs.

ID	*Gaia* Source ID	Periods (d) (G,A,O)	Amplitudes (mag) (BP,RP,G,V,I)	Comments
C1	5594538779611595136	(–,–, 0.7541)	(–,–,–,–, 0.18)	EW, MS
C2	5533487296963447552	(–, 0.2792,–)	(–,–,–, 0.23,–)	EW, MS
C3	2012045019718073728	(–, 0.4310,–)	(–,–,–, 0.18,–)	EW, MS
C4	2004077065120273664	(0.8335,–,–)	(0.21, 0.16, 0.18,–,–)	EW, MS
C5	5534158205211222144	(0.3622,–,–)	(0.80, 0.27, 0.27,–,–)	noisy, below-HB
C6	5585551027962400384	(–, 0.4400,–)	(–,–,–, 0.17,–)	EB, MS
C7	511219584907760896	(–, 0.4992,–)	(–,–,–, 0.13,–)	off-MS, short Amp
C8	5294043694838471552	(–, 0.7017,–)	(–,–,–, 0.09,–)	EB, MS
C9	5616530661434711680	(–,–, 0.7728)	(–,–,–,–, 0.17)	EB, MS
C10	5957810991851847296	(–,–, 0.3583)	(–,–,–,–, 0.13)	EB, MS
C11	4085159414905583104	(–,–, 0.4053)	(–,–,–,–, 0.17)	EB, MS
		(PS1)	(g,r,i,z)	
C12	3355237350809737344	(0.2723)	(0.51, 0.36, 0.29, 0.19)	constant/EA?
		(ZTF)	(g,r)	
C13	182831054077294336	(0.8605)	(0.10,0.10)	constant/EA?
C14	3330383474578837248	(0.3134)	(0.19,0.12)	MS, below-HB

Appendix B: Extinction

Trumpler 5 is located in a region with high differential extinction. In Fig. B.1 we show the dependence of A_V as a function of distance along the line of sight to the RRL, for the Lallement et al. (2022) and Green et al. (2019) 3D extinction maps. The overall trend is very similar but there are localised differences up to ~0.25 mag between the two maps. At the RRL's distance the G19 map predicts larger extinction than the L22 map by ~0.15 mag.

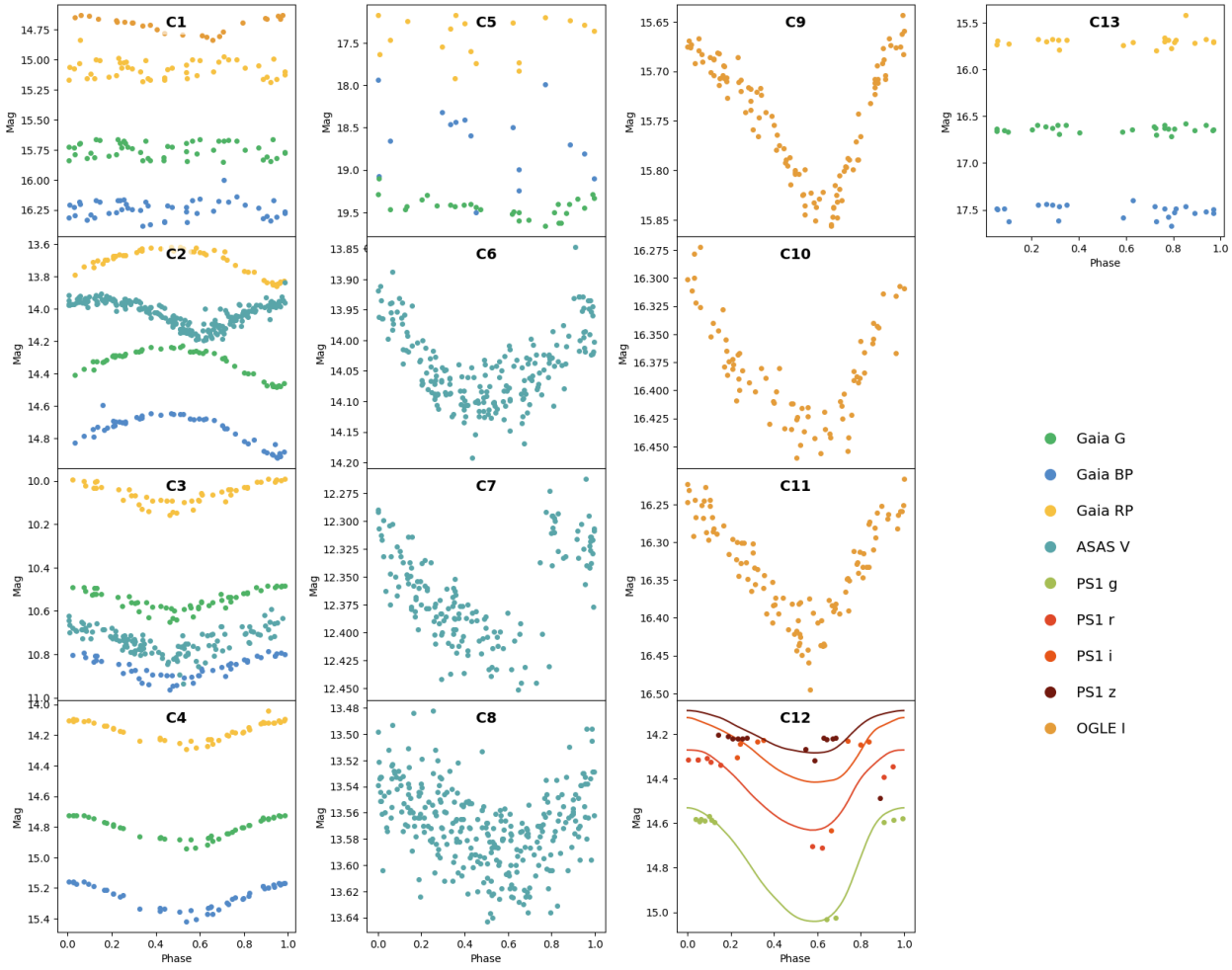

Fig. A.1. Phase-folded light curves for each of the 13 out of 14 stars discarded from the sample, with available time series data. Star 3330383474578837248 is not shown as it was identified by ZTF alone and its time series data is not publicly available, not does it have time series information in *Gaia* DR3.

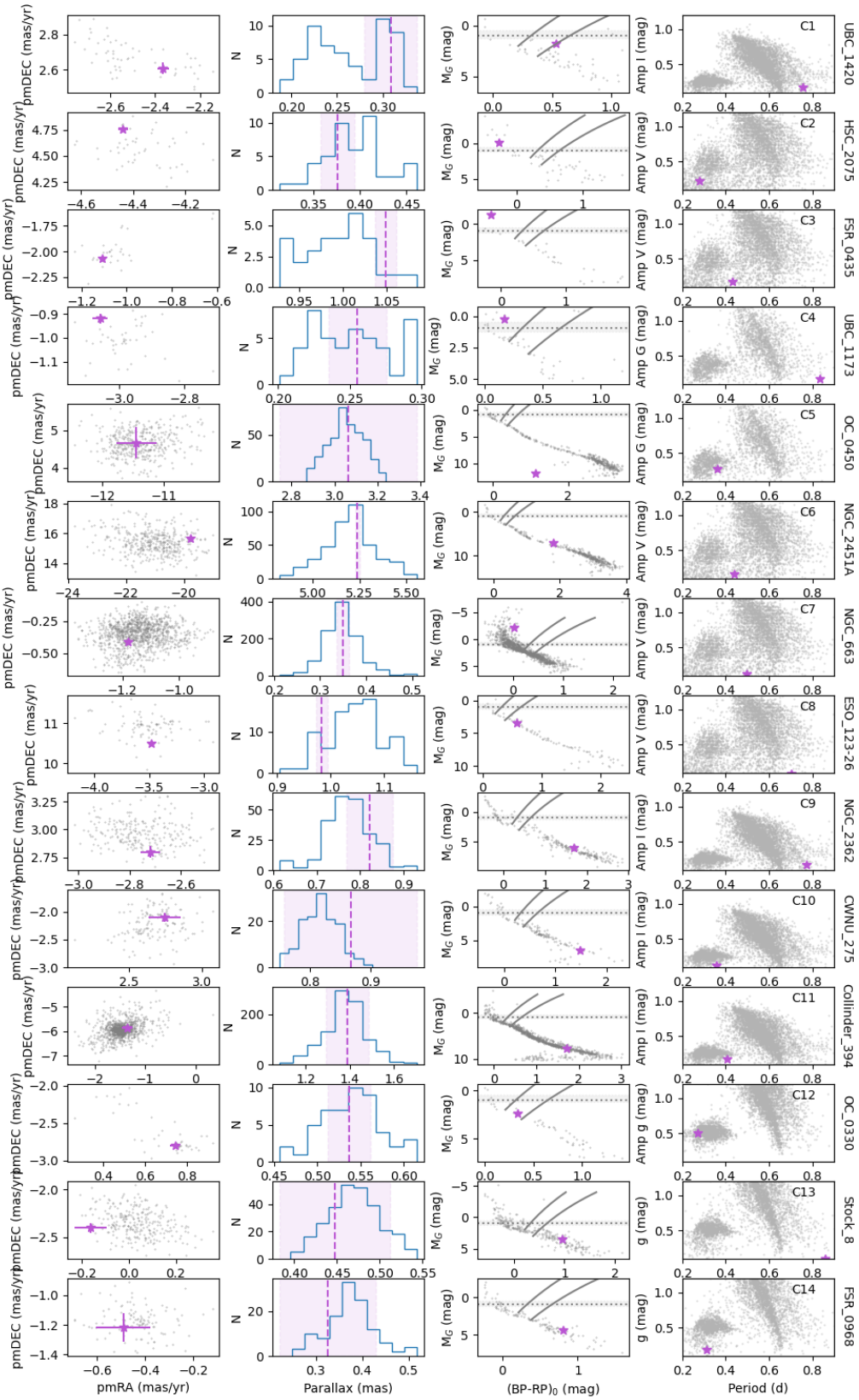

Fig. A.2. Discarded RRL stars (purple star) and cluster members (light gray) are shown, from left to right, in the plane of proper motions (pmDec versus pmRA), parallax, *Gaia* CAMD and Period-Amplitude diagram. In the CAMD, the solid lines correspond to IS limits from Marconi et al. (2015); the dotted line shows the expected location of the HB at each cluster's metallicity from Garofalo et al. (2022), and the absolute magnitude and intrinsic colours computed based on the distance and extinction according to Hunt & Reffert (2024); the shading represents the uncertainty in the HB luminosity corresponding to Δ[Fe/H] = 0.5 dex. The star's ID from Table A.1 and the cluster's name are shown in the fourth panel top right corner and Y axis, respectively.

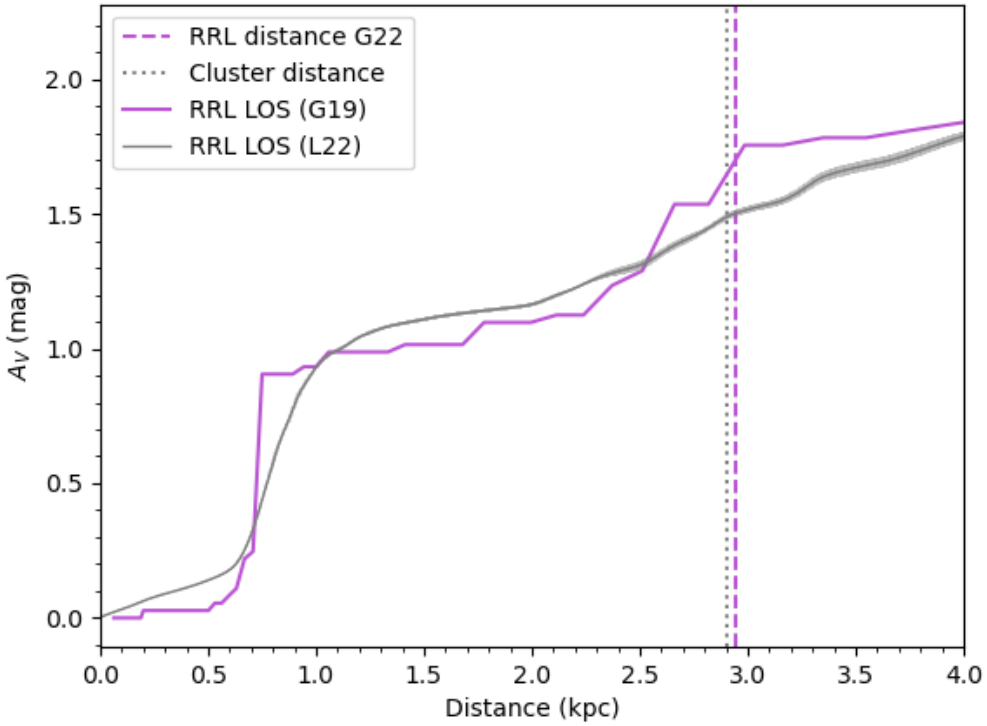

Fig. B.1. Extinction in the V band along the RRL's line of sight from the G19 and L22 extinction maps. The width of the L22 curve represents the 1σ uncertainty in extinction at fixed distance. The RRL's parallax distance and cluster's mean distance summarised in Table 1 are shown with the dashed and dotted lines respectively.